


# Circular RNA circCPA4 promotes tumorigenesis by regulating miR-214-3p/TGIF2 in lung cancer

Wenhu Tao<sup>1</sup>  | Cheng Cao<sup>1</sup> | Gaofei Ren<sup>2</sup> | Decun Zhou<sup>2</sup>

<sup>1</sup>Department of Thoracic Surgery, the First Affiliated Hospital of Anhui Medical University, Hefei, China

<sup>2</sup>Department of Cardiovascular Surgery, Anhui No. 2 Provincial People's Hospital, Hefei, China

## Correspondence

Wenhu Tao, Department of Thoracic Surgery, the First Affiliated Hospital of Anhui Medical University, No. 218, Jixi Road, Hefei 230031, Anhui, China.  
Email: wenhutao@126.com

## Funding information

Key Research Projects of Natural Science in Colleges and Universities of Anhui Province, Grant/Award Number: KJ2018A0858

## Abstract

**Background:** Lung cancer is the most prevalent malignancy in adults. Circular RNA (circRNA) circCPA4 (hsa\_circ\_0082374) is highly expressed in non-small cell lung cancer (NSCLC). The purpose of this study was to explore the role and mechanism of circCPA4 in lung cancer.

**Methods:** CircCPA4, linear CPA4, TGF- $\beta$ -induced factor homeobox 2 (TGIF2), and microRNA-214-3p (miR-214-3p) levels were measured by real-time quantitative polymerase chain reaction (RT-qPCR). The protein levels of TGIF2, Beclin1, and p62 were assessed by western blot assay. Colony numbers, migration, invasion, apoptosis, and cell cycle progression were examined by colony formation, wound-healing, transwell, and flow cytometry assays, respectively. The binding relationship between miR-214-3p and circCPA4 or TGIF2 was predicted by StarBase or TargetScan and then verified by a dual-luciferase reporter, RNA immunoprecipitation (RIP), and RNA pulldown assays. The biological role of circCPA4 on lung tumor growth was assessed by a xenograft tumor model in vivo, and TGIF2 and ki-67 expression was assessed by immunohistochemistry.

**Results:** We determined that CircCPA4 and TGIF2 were increased, and miR-214-3p was decreased in lung cancer tissues and cells. Functionally, circCPA4 knockdown could suppress colony formation, migration, invasion, cell cycle progression, and expedite apoptosis of lung cancer cells in vitro. Mechanically, circCPA4 could regulate TGIF2 expression by sponging miR-214-3p. In addition, circCPA4 deficiency inhibited the tumor growth in lung cancer in the mouse model.

**Conclusions:** CircCPA4 could act as a sponge of miR-214-3p to upregulate TGIF2 expression, thereby promoting the progression of lung cancer cells. These findings suggested underlying therapeutic targets for the treatment of lung cancer.

## KEYWORDS

CircCPA4, lung cancer, miR-214-3p, progression, TGIF2

## INTRODUCTION

Lung cancer is the most common malignant tumor in adults, accounting for a quarter of cancer deaths in the United States.<sup>1</sup> Genetic and environmental changes are thought to be associated with the cause of lung cancer, especially smoking.<sup>2,3</sup> Currently, surgery, radiotherapy, and chemotherapy are the main traditional methods for the

treatment of lung cancer. Despite the great progress in these methods, the prognosis of patients with lung cancer is still dismal due to the high rate of metastasis and recurrence.<sup>4</sup> Hence, identifying the effective therapeutic target and understanding the carcinogenesis of lung cancer are necessary for the development of alternative antilung cancer therapeutic strategies.

Circular RNAs (circRNAs) are a kind of endogenous non-coding transcripts that form a covalently closed loop without 5' caps and 3' polyadenylated tail.<sup>5</sup> Over the past

Wenhu Tao and Cheng Cao contributed equally to this work.

This is an open access article under the terms of the Creative Commons Attribution-NonCommercial License, which permits use, distribution and reproduction in any medium, provided the original work is properly cited and is not used for commercial purposes.

© 2021 The Authors. *Thoracic Cancer* published by China Lung Oncology Group and John Wiley & Sons Australia, Ltd.

few decades, a number of circRNAs have been identified as highly represented in mammalian cells caused by the development of high-throughput technology.<sup>6</sup> It has previously been reported that circRNAs participate in the regulation of gene expression at different levels.<sup>7</sup> Mounting evidence suggests that the dysregulation of circRNA has an inextricable connection with the initiation and development of lung cancers. It has also been reported that Hsa\_circRNA\_103809 works as a positive regulator in lung cancer development through interacting with miR-4302.<sup>8</sup> Gao et al. reported that the overexpression of hsa\_circ\_0007059 attenuates the malignancy of lung cancer through blocking proliferation and epithelial-mesenchymal transition (EMT).<sup>9</sup> Of note, circRNA circCPA4 (hsa\_circ\_0082374), a poor prognostic factor, has been linked to glioma proliferation and metastasis.<sup>10</sup> Furthermore, in non-small cell lung cancer (NSCLC), a recent publication documented that circCPA4 exerts an oncogene role via enhancing cell growth, mobility, and EMT.<sup>11</sup> However, the role of circCPA4 in lung cancer has not yet been fully elucidated.

Over the past several years, some researchers have reported that epigenetic factors such as microRNAs (miRNAs) might take part in tumorigenesis through modulating tumor growth and metastasis.<sup>12,13</sup> As another class of endogenous non-coding RNA with about 22 nts, miRNAs can regulate gene expression at the post-transcriptional level.<sup>14</sup> Previous studies have suggested that dysregulation of miRNAs is implicated in the progression of human cancers, serving as tumor-suppressive or oncogenic miRNAs.<sup>15</sup> MicroRNA-214-3p (miR-214-3p) has been reported to exhibit a repression role in a variety of human cancers, such as colon cancer,<sup>16</sup> osteosarcomas,<sup>17</sup> and hepatocellular carcinoma.<sup>18</sup> Moreover, it has been reported that miR-214-3p can hinder cell growth by binding to fibroblast growth factor receptor 1 (FGFR1) and 3-phosphoinositide-dependent protein kinase-1 (PDK1) in lung cancer cells,<sup>19,20</sup> suggesting a tumor-suppressive role of miR-214-3p in lung cancer.

As a transcription regulator, TGF- $\beta$ -induced factor homeobox 2 (TGIF2) has been verified to be linked to the regulation of development and progression in various cancers.<sup>21,22</sup> In terms of lung cancer, it has been reported that TGIF2 promotes the progression of lung adenocarcinoma by regulating EGFR/RAS/ERK signaling.<sup>23</sup> Also, the upregulation of TGIF2 could aggravate the malignancy of tumors in NSCLC cells by boosting proliferation, migration, and invasion.<sup>24</sup> A study by Pang et al. indicated that miR-449a could curb cell growth and metastasis of NSCLC by targeting TGIF2.<sup>25</sup> These reports therefore imply that TGIF2 plays a vital role in lung cancer progression.

Here, this study verified that circCPA4 and TGIF2 were increased, and their downregulation depressed cell growth, metastasis, and autophagy of lung cancer, respectively. Bioinformatic analysis validated that miR-214-3p could interact with circCPA4 or TGIF2. Hence, we put forward the hypothesis that the regulatory role of circCPA4 might be mediated by the miR-214-3p/TGIF2 axis.

## METHODS

### Clinical samples and cell culture

The approval of this research was endowed by the Ethics Committee of the First Affiliated Hospital of Anhui Medical University (approval number: Quick-PJ 2012-05-27) and was carried out according to the guidelines of the Declaration of Helsinki. NSCLC tissues and nontumor adjacent tissues were collected from 33 lung cancer patients without any treatment prior to surgery at the First Affiliated Hospital of Anhui Medical University from January 2012 to June 2015. The clinicopathological features of these patients are shown in Table 1. All participants signed their written informed consent.

Lung cancer cell lines (A549, NCI-H1299, SK-MES-1, and Calu-3) were purchased from American Type Culture Collection (ATCC, Manassas), and human bronchial epithelial cells (16HBE) were provided by Sigma-Aldrich. Under an incubator with 5% CO<sub>2</sub> at 37°C, all cells were routinely grown in Dulbecco's modified Eagle's medium (DMEM; Gibco). Then, 10% fetal bovine serum (FBS; Tianhang Biotechnology) was added to the medium and 1% penicillin/streptomycin (Gibco).

### Real-time quantitative polymerase chain reaction (RT-qPCR)

Based on the operation manual of the TRIzol reagent (Invitrogen), total RNA from tissues and cell lines was extracted. Thereafter, the isolated RNA was reversely transcribed with a PrimeScript RT Reagent Kit (TaKaRa). Then, on the Cycler CFX6 System (Applied Biosystems), SYBR Green PCR Kit (Takara, for circRNA and mRNA), and a TaqMan MicroRNA Assay Kit (Applied Biosystems, for miRNA) were used for the RT-qPCR assay. The obtained data were calculated by the  $2^{-\Delta\Delta C_t}$  method after normalization with endogenous controls: glyceraldehyde 3-phosphate dehydrogenase (GAPDH for CircCPA4, CPA4, TGIF2), and U6 (for miR-214-3p). RT-qPCR assay was performed at least three times. The primer sequences are presented in Table 2.

### Ribonuclease R (RNase R) assay

Briefly, the experiment was performed at 37°C for 15 min through incubating 1  $\mu$ g of total RNA with or without 3 U of RNase R (Epicenter). After that, treated RNA was subjected to RT-qPCR analysis of circCPA4 and linear CPA4. In addition, Sanger sequencing (Sangon) of a PCR product resulting from divergent primers demonstrates the head-to-tail splicing of this exon.

### Western blot assay

For total protein preparation, tissues and cells were treated with precold RIPA buffer (Beyotime) including protease

**TABLE 1** Correlation of clinicopathological features of lung cancer patients with circCPA4 expression levels

Characteristics	All cases	circCPA4 expression		<i>p</i> -value
		High	Low	
Age				0.4905
≥60	19	11	8	
<60	14	6	8	
Gender				0.1663
Male	18	7	11	
Female	15	10	5	
Smoking				0.4813
Yes	13	8	5	
No	20	9	11	
Tumor size (cm)				0.0039
≥5	13	11	2	
<5	20	6	14	
Histological type				0.0820
Squamous	8	6	2	
Adenocarcinoma	16	9	7	
Large cell lung cancer	9	2	7	
Lymph node metastasis				0.0494
Negative	19	7	12	
Positive	14	10	4	
TNM stage				0.0185
I–II	20	7	13	
III–IV	13	10	3	
Surgical resection				0.4117
Sublobar resection	6	4	2	
Lobectomy	27	13	14	
Tumor location				0.5133
Left lung	13	6	7	
Right lung	20	11	8	

inhibitor (cocktail, Roche, Basel, Switzerland). For immunoblotting, 50 µg protein samples were processed, separated using an SDS-PAGE system, transferred onto nitrocellulose membranes (Millipore), blocked in 5% skim milk for 2 h, hybridized with primary antibodies against TGIF2 (1:1000, ab155948, Abcam), Beclin1 (1:1000, ab210498, Abcam), p62 (1:1000, ab109012, Abcam), and GAPDH (1:1000, ab9485, Abcam), and incubated with a secondary antibody (ab205718, 1:10000, Abcam). Finally, the ECL detection system (GE Healthcare) was used for visualization, and Image J software (National Institutes of Health, Bethesda, MD, USA) was employed for analysis. Western blot assay was carried out at least three times.

## Cell transfection

In this assay, RiboBio provided circCPA4 small interfering RNA (si-circCPA4#1, #2), si-TGIF2 (#1, #2), and their

**TABLE 2** The sequences of primers for RT-qPCR used in this study

Names	Sequences (5'-3')
CircCPA4: Forward	ACAGCATCTGGTGTGTGCTT
CircCPA4: Reverse	CCCTTCTCTGCAAACTAGC
Linear CPA4: Forward	ATTGGACATTCGTTGAAAACCG
Linear CPA4: Reverse	ACGGGAGATCCACTCTCGGGA
TGIF2: Forward	TCTCTGTGTTGCCTCCCTCT
TGIF2: Reverse	CCACCTCAGCCCAATACACT
MiR-214-3p: Forward	GCGACAGCAGGCACAGACA
MiR-214-3p: Reverse	AGTGCAGGGTCCGAGGTATT
U6: Forward	CTCGCTTCGGCAGCACA
U6: Reverse	AACGCTTACGAATTTGCGT
GAPDH: Forward	GTGGACCTGACCTGCCGTCT
GAPDH: Reverse	GGAGGAGTGGGTGTCGCTGT

scrambled siRNA control (si-NC), miR-214-3p mimic (miR-214-3p), miR-214-3p inhibitor (in-miR-214-3p) and their negative controls (miR-NC and in-miR-NC), and circCPA4 overexpression (circCPA4) and its control (vector). TGIF2 (Accession: ABO42646.1) overexpression vector was constructed by inserting the sequence of TGIF2 into pcDNA vector (Invitrogen) with BamH I and Xho I sites, and the pcDNA empty vector (Invitrogen) was the corresponding control (pcDNA). A549 and NCI-H1299 cells were cultured to 60%–70% confluence. Subsequently, using lipofectamine 3000 reagent (Invitrogen), the oligonucleotides (50 nM) or vectors (200 ng) were transfected into the lung cell lines for 48 h.

## Colony formation assay

Transfected cells ( $5 \times 10^2$  cells/well) in 6-well plates were cultured for 1–2 weeks at 37°C. After discarded the supernatants, the numbers of colonies per well were fixed with methyl alcohol for 15 min at –20°C, and stained with crystal violet (Sigma-Aldrich) for 20 min. At last, visible colonies were imaged and counted manually. The experiment was conducted three times.

## Wound healing and transwell assays

For the wound healing assay, transfected A549 and NCI-H1299 cells were cultured in 6-well plates and allowed to grow to a confluence of 90% overnight. After scratching with a 200 µl sterile pipette tip (record 0 h) to create a clear cell-free zone, the cells in serum-free medium were incubated for 24 h. Cell migration was photographed using a light microscope (Nikon, magnification  $\times 100$ ), and the distance of 0–24 h was examined with Image J software (National Institutes of Health). This assay was carried out at least three times.

For transwell assay,  $2 \times 10^5$  transfected cells in the medium with 1% FBS were added into the upper chamber (BD Bioscience) with matrigel-precoated inserts (BD Bioscience). Thereafter, the lower counterpart was full of the medium with 20% FBS overnight. Finally, cells which had invaded into the lower counterpart were stained with 0.1% crystal violet (Sigma-Aldrich). The number of invaded cells was detected using an inverted microscope (Nikon, magnification $\times 100$ ). The assay was performed in triplicate.

### Cell apoptosis and cell cycle assay

For the measurement of the cell apoptosis rate, Annexin (V-fluorescein isothiocyanate) V-FITC/propidium iodide (PI) (Beyotime) was utilized in lung cancer cells. In brief, transfected A549 and NCI-H1299 cells were collected and washed with PBS (Invitrogen). Then, treated cells were incubated with 100  $\mu$ l binding buffer containing 5  $\mu$ l of an equal amount of Annexin V-FITC/PI (Beyotime). FACSCalibur (BD Bioscience) was conducted to analyze the results of apoptosis. For assessment of cell cycle progression, transfected cells were treated with PBS (Invitrogen) twice, followed by fixation with ethanol. After additional incubation with RNase A (Sigma-Aldrich) for 30 min, treated cells were incubated with PI for 30 min at room temperature. The percentages of cells in the G0-G1, S, and G2-M phases were detected according to the FACSCalibur flow cytometry (BD Biosciences). This assay was carried out at least three times.

### Dual-luciferase reporter assay

The binding between miR-214-3p and circCPA4 or TGIF2 was respectively predicted by StarBase (<http://starbase.sysu.edu.cn/>) or TargetScan (<http://www.targetscan.org/>), as proved by dual-luciferase reporter assay. Generally, the fragment of circCPA4 and TGIF2 3'UTR harboring wild-type (WT) or mutant-type (MUT) putative miR-214-3p binding sites were synthesized and inserted into the SaII and XbaI restriction sites in the pmirGLO vector (Promega). The constructed reporter plasmids were cotransfected with miR-214-3p or miR-NC into A549 and NCI-H1299 cells, followed by incubation for 48 h. The luciferase activity was assessed in line with the instructions of dual-luciferase reporter assay kit (Promega), and firefly luciferase activity was normalized to Renilla activity. Luciferase reporter assay was performed at least three times.

### RNA immunoprecipitation (RIP)

After the A549 and NCI-H1299 cell confluency reached 80%, the lung cancer cells were collected and lysed in the complete RIP lysis buffer. Cell extracts were subsequently incubated with magnetic beads conjugated with

anti-Argonaute 2 antibody (Anti-Ago2; Millipore) or negative control normal mouse IgG (Millipore) overnight at 4°C, and were then digested with proteinase K (Invitrogen). The immunoprecipitated RNAs were purified with RNeasy MinElute Cleanup Kit (Qiagen), followed by analysis using RT-qPCR assay. The assay was performed in triplicate.

### RNA pulldown assay

A549 and NCI-H1299 cells were transfected with 50 nM biotinylated Bio-miR-214-3p probe (Sangon) or the negative control Bio-con (Sangon) for 48 h, followed by collection. After incubation in lysis buffer, the cell lysates were subjected to M-280 streptavidin magnetic beads (Sigma-Aldrich), and cultured for another 3 h. The bound RNA was purified and subjected to RT-qPCR reaction to gauge circCPA4 and TGIF2 enrichment. The assay was conducted at least three times.

### Tumor xenograft assay

BALB/C nude mice (male, 4–5 weeks old, and 18–20 g weight) were purchased from Vital River Laboratory (Beijing, China), and then kept in a pathogen-free environment. CircCPA4 knockdown stable lentiviral vector (lenti-short hairpin-circCPA4, sh-circCPA4), stable overexpression vector (oe-circCPA4), and the corresponding control (sh-NC, vector) were provided by GeneChem (Shanghai, China). The mice were then randomly divided into four groups (5 in each group) and injected with NCI-H1299 cells transfected with sh-circCPA4, sh-NC, oe-circCPA4, or vector. In summary, after suspension in 200  $\mu$ l PBS, NCI-H1299 cells ( $5 \times 10^6$ ) were subcutaneously injected into the back flanks of the mice, followed by measurement of tumor volume at the indicated time points (7, 14, 21, 28 days) after the first injection. Four weeks after implantation, all mice were subjected to euthanasia using an isoflurane overdose, and the tumor tissues were surgically excised. They were then imaged and weighed, followed by RT-qPCR and western blot analysis. In addition, immunohistochemistry staining was conducted as described previously.<sup>26</sup> In brief, the tissue samples from xenograft tumors were fixed in 10% neutral buffer formalin, dehydrated, and embedded in paraffin. Thereafter, the samples were sectioned at a 5  $\mu$ m thickness, which was treated with biotinylated secondary antibody, followed by the addition of the chromogen. Finally, slides were counterstained with hematoxylin, followed by analysis of histopathology under a microscope. In order to detect the levels of TGIF2 and ki-67 in excised xenograft tumors, the sections were washed with PBS and probed with primary antibody TGIF2 (ab190152, Abcam) and ki-67 (ab16667, Abcam) and then with horseradish peroxidase-conjugate streptavidin (ab205718, Abcam) and Biotinylated secondary antibody. Finally, protein levels were analyzed by calculating the integrated optical

density per stained area using Image-Pro Plus 6.0 software (Media Cybernetics). According to the percentage of dyeing positive cells (A), the dyeing positive cell number of zero was 0, <30% was 1, 30%–60% was 2, and >60% was 3. According to the dyeing intensity (B), the achromatic color was 0, the weak dyeing was 1, the dyeing was 2, and the strong dyeing was 3; the total score (A + B)  $\geq$  3 divides into the positive expression, and <3 divides into the negative expression. This animal experiment received the approval of the Animal Ethics Committee of the First Affiliated Hospital of Anhui Medical University (approval number: Quick-dsy 2016-03-13) and was performed in accordance with the guidelines of the National Animal Care and Ethics Institution.

## Statistical analysis

GraphPad Prism7 software was employed to analyze all data. The measurement of data is shown as mean  $\pm$  standard deviation (SD) from three independent experiments. The expression association between miR-214-3p and circCPA4 or TGIF2 was assessed using Pearson's correlation analysis. Data comparison between two groups or more than two groups was analyzed using Student's *t*-test or one-way analysis of variance (ANOVA) with Tukey's tests. A *p*-value less than 0.05 was considered statistically significant.

## RESULTS

### CircCPA4 and TGIF2 were elevated in lung cancer tissues and cells

At first, Sanger sequencing suggested that circCPA4 was derived from exons 7, 8, 9, and 10 of the CPA4 gene (Figure 1a). Then, we identified the expression pattern of circCPA4 in lung cancer by RT-qPCR assays. As shown in Figure 1b, the expression level of circCPA4 was increased in 33 NSCLC tissues compared with 33 adjacent normal tissues. To probe the association of circCPA4 expression with clinicopathological features, 33 patients with NSCLC were classified (Table 1). Data shows that circCPA4 expression was associated with tumor size, lymph node metastasis, and TNM stage (*p* < 0.05). Additionally, the Kaplan–Meier survival curves demonstrated that the lung cancer patients in low circCPA4 level group had a higher survival rate than those in high circCPA4 level group (Figure 1c). Then, we further verified the upregulation of circCPA4 in lung cancer cell lines (A549, NCI-H1299, SK-MES-1, and Calu-3) relative to the human bronchial epithelial cell line (16HBE) (Figure 1d). Upregulation was evident particularly in A549 and NCI-H1299 cells, and these two cell lines were selected for the following experiments. Also, to detect the stability of circCPA4, A549 and NCI-H1299 cells were treated with RNase R. Data suggested that the treatment of RNase R reduced the RNA level of linear CPA4, whereas had no

obvious effect on circCPA4 (Figure 1e,f). Moreover, we observed that TGIF2 was also higher in NSCLC tissues than normal tissues (Figure 1g,i). Meanwhile, immunohistochemical staining also showed that the expression of ki-67 (a proliferation-related marker) was apparently increased in the NSCLC tissues compared with the adjacent normal tissues (Figure 1h). Of interest, the trend of TGIF2 mRNA and protein level in lung cancer lines was in line with that in lung cancer tissues (Figure 1j,k). In a word, the dysregulation of circCPA4 and TGIF2 might be associated with the progression of lung cancer.

### CircCPA4 knockdown inhibited colony formation, migration, invasion, cell cycle progression, and expedited apoptosis of lung cancer cells

Then, to explore the biological function of circCPA4 in lung cancer development, we conducted circCPA4 silencing experiments in A549 and NCI-H1299 cells. As shown in Figure 2a,b, circCPA4 level was apparently decreased in si-circCPA4#1 or si-circCPA4#2-transfected A549 and NCI-H1299 cells in comparison with cell transfected with si-NC, and the knockdown efficiency of si-circCPA4#2 is more obvious. Meanwhile, there had no evident effect on linear CPA4 mRNA in si-circCPA4#1 or si-circCPA4#2-transfected A549 and NCI-H1299 cells. So we chose si-circCPA4#2 for the functional experiments. Results showed that the knockdown of circCPA4 repressed the number of colonies in A549 and NCI-H1299 cells relative to the control groups (Figure 2c). Meanwhile, wound healing and transwell assays showed that the capabilities of migration and invasion in A549 and NCI-H1299 cells were suppressed due to the downregulation of circCPA4 versus their counterparts (Figure 2d,e). After that, compared with the control groups, the promotion of apoptosis rate was viewed due to the introduction of si-circCPA4#2 in A549 and NCI-H1299 cells (Figure 2f). Simultaneously, cell cycle results indicated that the cells in the si-circCPA4#2 group had an arrested cell cycle with a higher proportion of G0/G1-phase, and a lower proportion of S-phase when compared to that control groups (Figure 2g, h). It has previously been reported that autophagy plays a vital role in the development of lung cancer.<sup>27</sup> Hence, we next detected the autophagy-related proteins Beclin1 (proautophagy protein) and p62 (autophagy inhibitor) in lung cancer cells. As shown in Figure 2i, an enhanced Beclin1 protein level and declined p62 protein level was observed due to the downregulation of circCPA4. All these data suggested that the knockdown of circCPA4 could suppress the development and progression of lung cancer in vitro.

### MiR-214-3p interacted with circCPA4 or TGIF2 in lung cancer cells

Using the bioinformatic software StarBase or TargetScan, we found that there were some complementary sites between

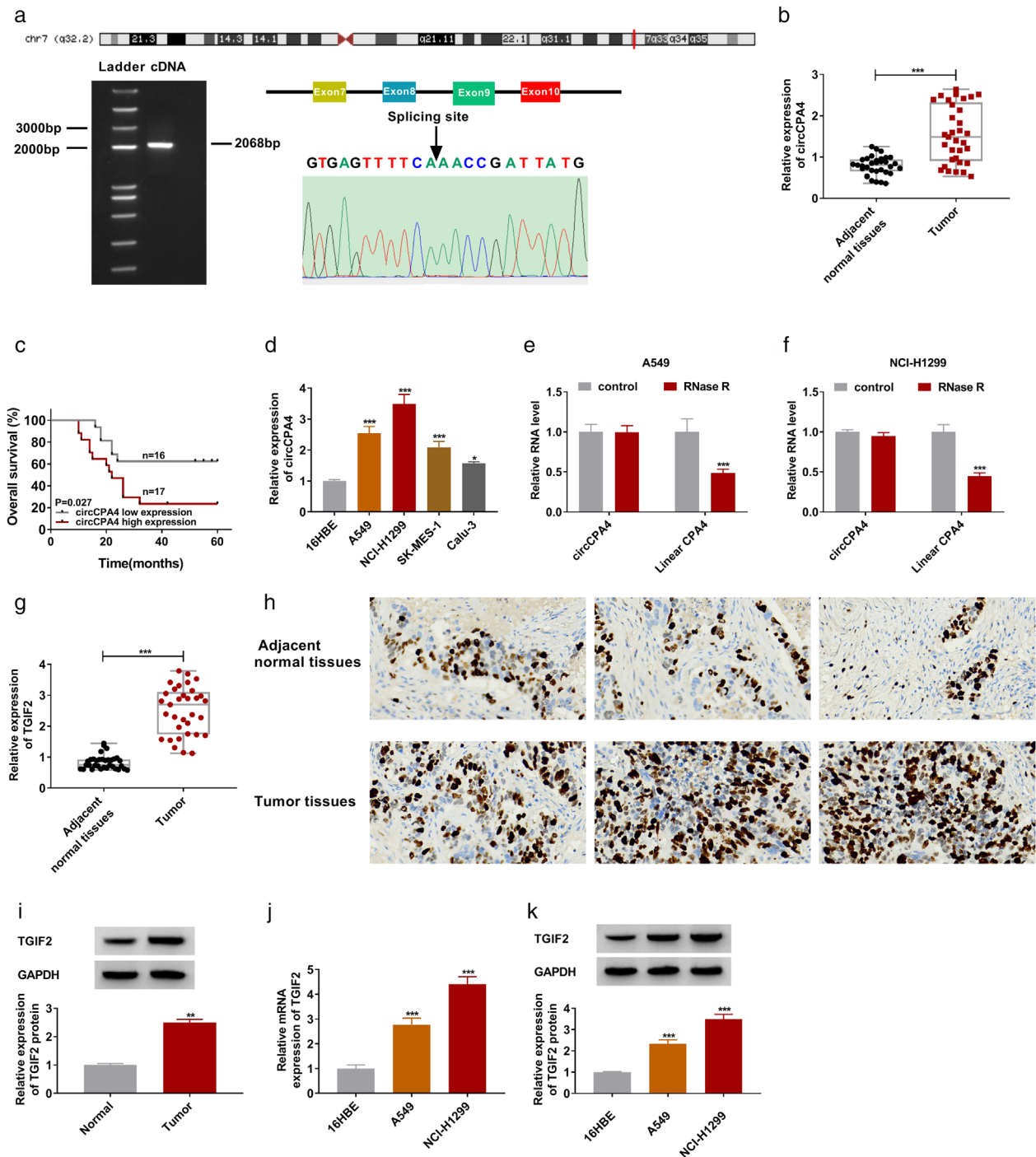


**FIGURE 1** Expression patterns of circCPA4 and TGIF2 in non-small cell lung cancer (NSCLC) tissues and cells. (a) The expression of circCPA4 was validated by Sanger sequencing. The black arrows on the left represent the back-splicing site of circCPA4. Also, circCPA4 is derived from back-splicing of exons 7, 8, 9, and 10 of the CPA4 gene. PCR product of circCPA4 in agarose gel electrophoresis and the splicing site verified by DNA sequencing. (b) Relative expression of circCPA4 was detected in 33 NSCLC tissues and 33 adjacent normal tissues by RT-qPCR assay. (c) The overall survival of HCC patients with circCPA4 high or low level was determined by Kaplan–Meier analysis. (d) CircCPA4 level was measured in human bronchial epithelial cell line (16HBE), and lung cancer cell lines (A549, NCI-H1299, SK-MES-1, and Calu-3). (e and f) Relative RNA levels of circCPA4 and linear CPA4 were examined in A549 and NCI-H1299 cells treated with or without RNase R. (g and i) TGIF2 levels were tested in 33 NSCLC tissues and 33 adjacent normal tissues by RT-qPCR and western blot assays. (h) Immunohistochemical staining analysis of ki-67 expression in NSCLC tissues and adjacent normal tissues. (j and k) The mRNA level and protein level of TGIF2 were assessed in 16HBE, A549, and NCI-H1299 cells. Values are presented as mean  $\pm$  SD,  $n = 3$ . \* $p < 0.05$ , \*\* $p < 0.01$ , \*\*\* $p < 0.001$

miR-214-3p and circCPA4 or TGIF2 (Figure 3a,b). A dual-luciferase reporter assay was then used to verify the prediction. As shown in Figure 3c,d, overexpression of

miR-214-3p could evidently reduce the luciferase activity of circCPA4 WT reporter, while had no effect on the luciferase activity of circCPA4 MUT reporter in A549 and

NCI-H1299 cells. Also, to further prove the direct binding relationship between circCPA4 and miR-214-3p, RIP assay was employed using antibody Ago2, which is an important component of RISC complex. Results indicated that both circCPA4 and miR-214-3p were notably enriched in the Anti-Ago2 groups relative to the Anti-IgG groups (Figure 3e,f). In agreement with the bioinformatic analysis, luciferase reporter, RIP assays, RNA pull-down results suggested that circCPA4 enrichment in the Bio-miR-214-3p probe group was significantly intensified compared with the Bio-con group, implying the interaction between circCPA4 and miR-214-3p (Figure 3g). These data verified that miR-214-3p was a direct target of circCPA4. Next, to further identify the interaction between miR-214-3p and TGIF2,

luciferase reporter, RIP, and RNA pull-down assays were carried out in lung cancer cells. As shown in Figure 3h,i, the luciferase activity of TGIF2 3'UTR WT was decreased in A549 and NCI-H1299 cells after the introduction of miR-214-3p mimics; however, the mutation in targeted sites significantly eliminated the influence of miR-214-3p upregulation on the reporter gene expression. Meanwhile, the results of the RIP assay suggested that miR-214-3p and TGIF2 in the Anti-Ago2 groups were higher than that in the Anti-IgG groups (Figure 3j,k). Also, compared with the Bio-con group, the remarkable enhancement of TGIF2 enrichment was viewed in the Bio-miR-214-3p probe group (Figure 3l). In addition, we further verified that miR-214-3p was expressed at a low level in NSCLC tissues and cell lines

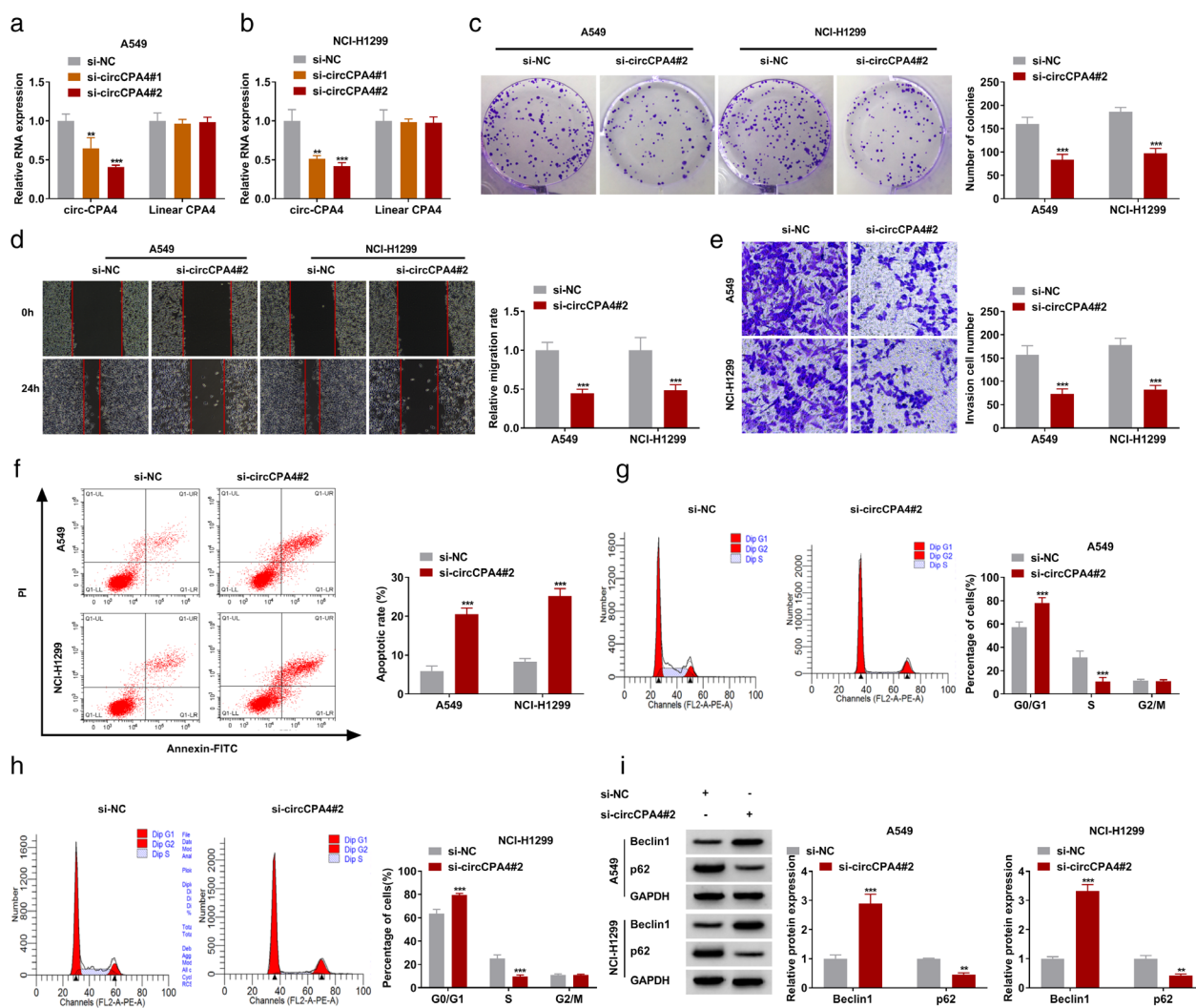


**FIGURE 2** Silencing of circCPA4 repressed colony formation, migration, invasion, cell cycle progression, and promoted apoptosis and autophagy of lung cancer cells. (a and b) CircCPA4 level and linear CPA4 mRNA level were detected in A549 and NCI-H1299 cells transfected with si-NC, si-circCPA4#1, and si-circCPA4#2. (c) Cell colony formation assay was employed to assess the colony formation number in si-NC or si-circCPA4#2-transfected A549 and NCI-H1299 cells. (d) Wound healing assay was carried out to detect migration rate in si-NC or si-circCPA4#2-transfected A549 and NCI-H1299 cells. (e) A transwell assay was conducted to evaluate invasion ability in si-NC or si-circCPA4#2-transfected A549 and NCI-H1299 cells. (f) Flow cytometry assay was performed to examine apoptosis rate in si-NC or si-circCPA4#2-transfected A549 and NCI-H1299 cells. (g and h) Cell cycle distribution was analyzed in si-NC or si-circCPA4#2-transfected A549 and NCI-H1299 cells using flow cytometry assay. (i) Western blot assay was used to detect the protein levels of Beclin1 and p62 in si-NC or si-circCPA4#2-transfected A549 and NCI-H1299 cells. Data are presented as mean  $\pm$  SD,  $n = 3$ . \*\* $p < 0.01$ , \*\*\* $p < 0.001$

versus their respective controls (Figure 3m,n). Taken together, the relationship between circCPA4 and TGIF2 might be mediated via miR-214-3p in lung cancer cells.

## TGIF2 downregulation repressed malignant behavior of lung cancer cells

Furthermore, we performed in vitro loss-of-function analyses to verify the effects of TGIF2 on lung cancer

progression. At first, the transfection efficiency of si-TGIF2#1 and si-TGIF2#2 were detected and presented in A549 and NCI-H1299 cells (Figure 4a,b). Considering the more significant transfection efficiency of Si-TGIF2 #2, it was selected for the subsequent experiments. Whereafter, colony formation assay displayed that the downregulation of TGIF2 could apparently hinder the number of colonies in A549 and NCI-H1299 cells (Figure 4c). Synchronously, reduced migration and invasion were noticed due to the knockdown of TGIF2 in A549 and NCI-H1299 cells

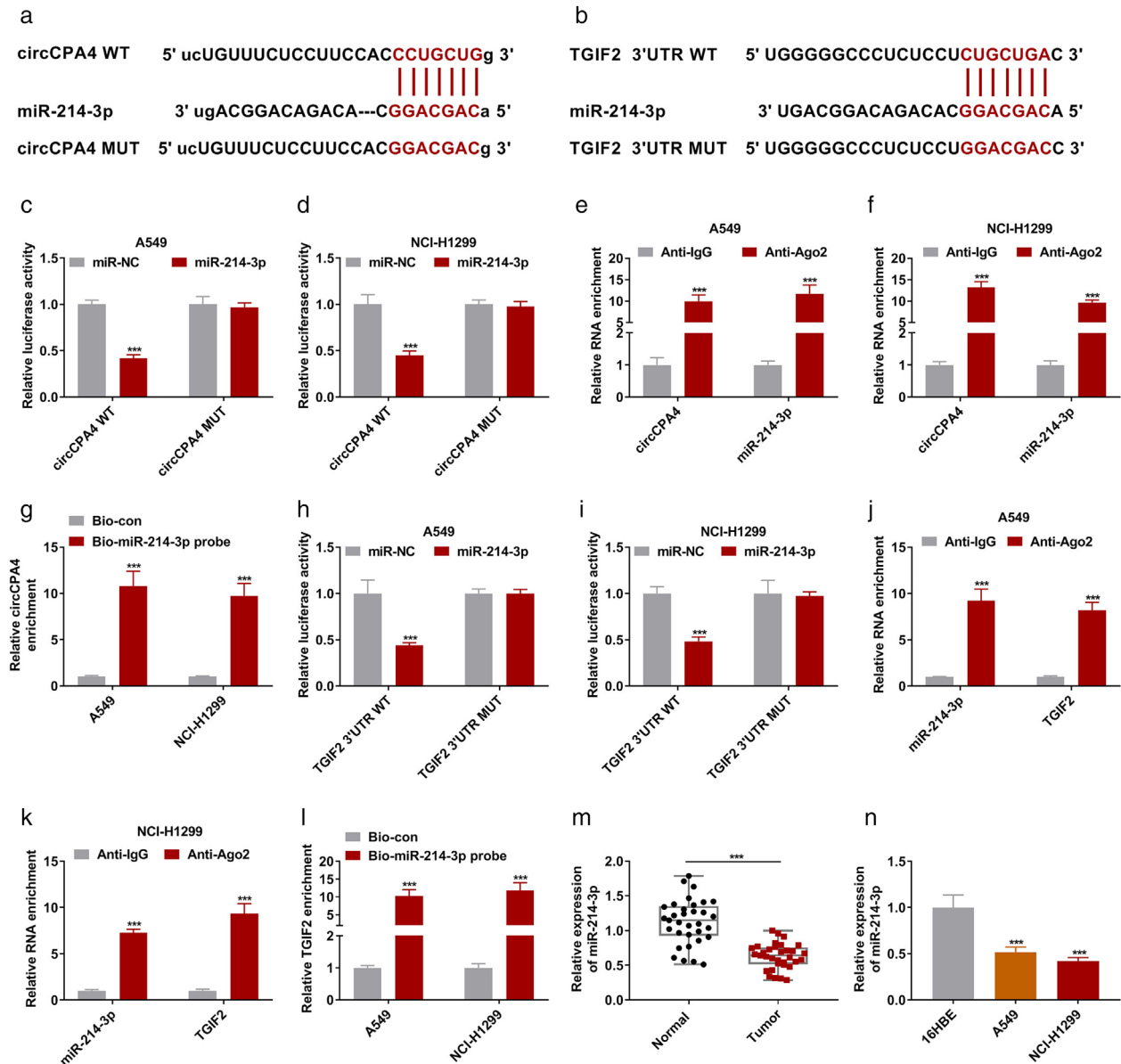


**FIGURE 3** CircCPA4 worked as a molecular sponge of miR-214-3p to sequester miR-214-3p away from TGIF2 in lung cancer cells. (a) The binding sites between circCPA4 and miR-214-3p were predicted by StarBase. (b) Putative binding sequences between miR-214-3p and TGIF2 3'UTR WT, and mutant sites in TGIF2 3'UTR reporter. (c and d) A dual luciferase reporter assay was applied to verify the prediction between circCPA4 and miR-214-3p. (e and f) RIP assay was performed in A549 and NCI-H1299 cell extracts to assess miR-214-3p endogenously correlated with circCPA4. (g) RNA pull-down assay was employed to prove the interaction between circCPA4 and miR-214-3p in A549 and NCI-H1299 cells. (h and i) The effects of miR-214-3p upregulation on luciferase activity of TGIF2 3'UTR WT and TGIF2 3'UTR MUT reporters were detected in A549 and NCI-H1299 cells. (j and k) The relationship between miR-214-3p and TGIF2 3'UTR was validated by RIP assay. (l) RNA pull-down assay was used to verify the interaction between miR-214-3p and TGIF2 3'UTR. (m and n) MiR-214-3p level was determined in non-small cell lung cancer tissues and cell lines (A549 and NCI-H1299), and their respective counterparts. Data are presented as mean  $\pm$  SD,  $n = 3$ . \*\*\* $p < 0.001$



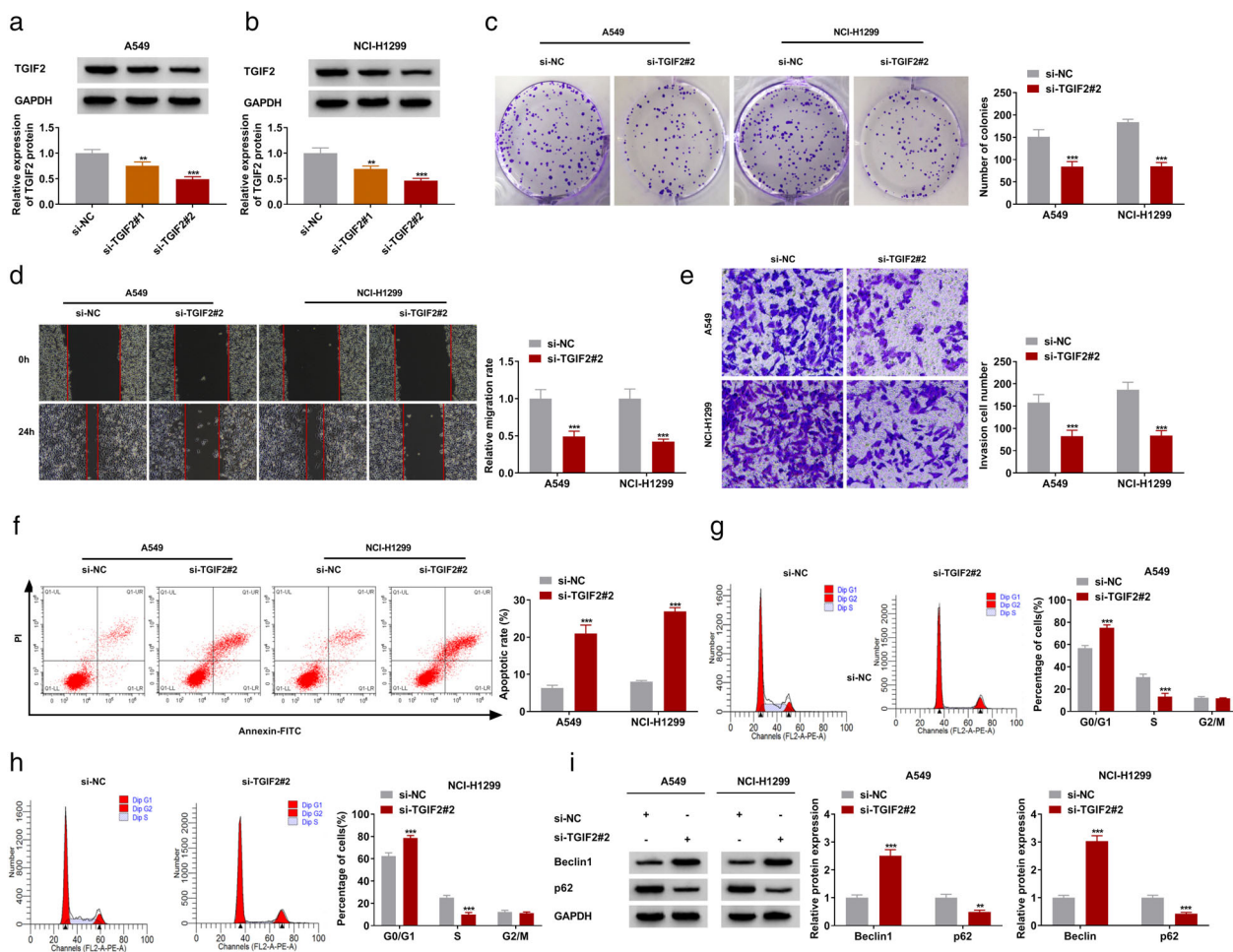


**FIGURE 4** The downregulation of TGIF2 led to a decrease in colony formation, migration, invasion, cell cycle progression, and an enhancement of apoptosis and autophagy in lung cancer cells. (a and b) TGIF2 protein level was assessed in A549 and NCI-H1299 cells transfected with si-NC, si-TGIF2#1, and si-TGIF2#2. (c) Number of colonies was calculated in si-NC or si-TGIF2#2-transfected A549 and NCI-H1299 cells. (d and e) The capabilities of migration and invasion were monitored in si-NC or si-TGIF2#2-transfected A549 and NCI-H1299 cells. (f) Apoptosis rate was tested in si-NC or si-TGIF2#2-transfected A549 and NCI-H1299 cells. (g and h) Cell cycle distribution was detected in si-NC or si-TGIF2#2-transfected A549 and NCI-H1299 cells. (i) Protein levels of Beclin1 and p62 were evaluated in si-NC or si-TGIF2#2-transfected A549 and NCI-H1299 cells. Data are presented as mean  $\pm$  SD,  $n = 3$ . \*\* $p < 0.01$ , \*\*\* $p < 0.001$

(Figure 4d,e). In addition, a flow cytometry assay showed that the silencing of TGIF2 elicited a striking increase in the apoptosis rate (Figure 4f) and an apparent decrease in cell cycle progression (Figure 4g,h). In terms of autophagy, Beclin1 was enhanced and p62 was reduced in A549 and NCI-H1299 cells by TGIF2 downregulation (Figure 4i). All in all, these observations indicated that the downregulation of TGIF2 could decline cell proliferation, migration, invasion, and promote apoptosis of lung cancer cells.

### TGIF2 upregulation overturned the inhibitory impact of circCPA4 knockdown on the progression of lung cancer

Next, we further analyzed the effects of circCPA4 on TGIF2 expression in lung cancer cells. First, RT-qPCR and western blot assays were used to detect the overexpression efficiency

of TGIF2 in A549 and NCI-H1299 cells. Data revealed that TGIF2 level was significantly upregulated in TGIF2-transfected A549 and NCI-H1299 cells when compared with empty vector controls (Figure 5a,b). Furthermore, restoration experiments indicated that the knockdown of circCPA4 repressed the mRNA and protein levels of TGIF2, which was significantly mitigated by the upregulation of TGIF2 (Figure 5c–e). Functional analysis suggested that the repression of colony formation (Figure 5f) due to the deficiency of circCPA4 was abrogated by the introduction of TGIF2 in A549 and NCI-H1299 cells. Meanwhile, our data also indicated that the reintroduction of pcDNA-TGIF2 could obviously overturn the negative role of circCPA4 downregulation on migration (Figure 5g), and invasion (Figure 5h) in A549 and NCI-H1299 cells. Synchronously, the overexpression of TGIF2 could reverse the inductive role of circCPA4 silencing on apoptosis rate (Figure 5i) and cell cycle arrest (Figure 5j,k) in A549 and

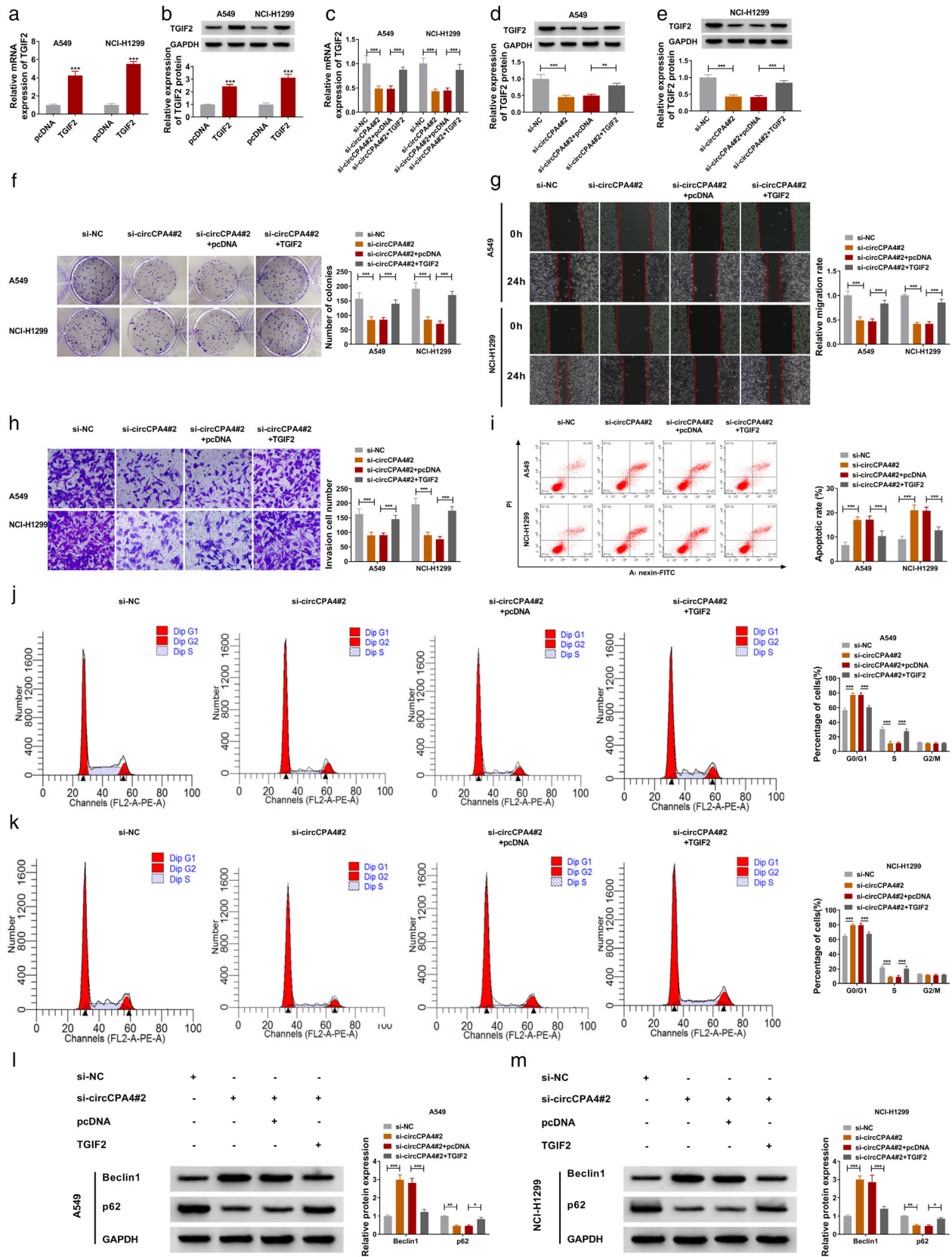
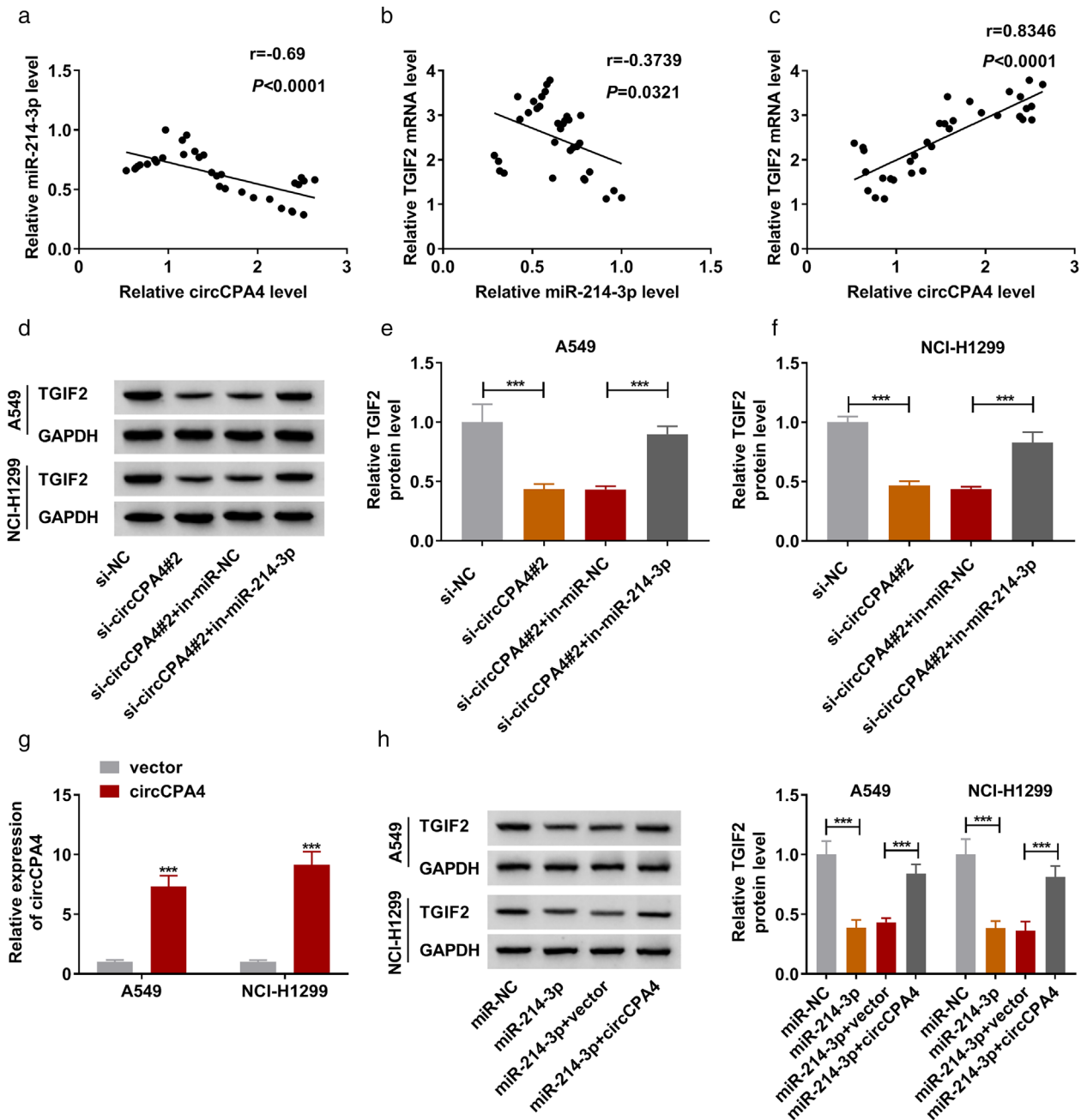
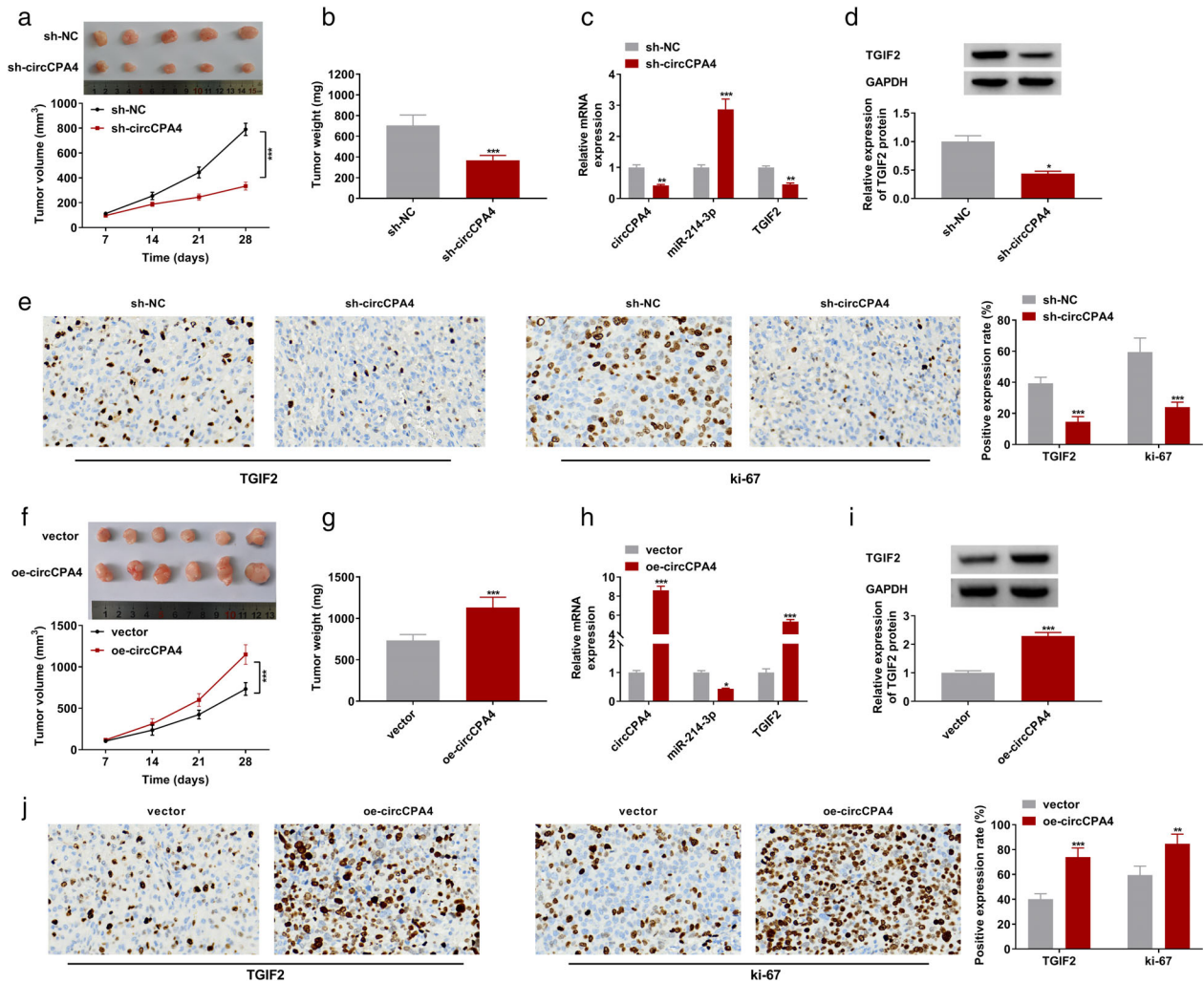


FIGURE 5 Legend on next page.



**FIGURE 6** Validation of circCPA4/miR-214-3p/TGIF2 axis in lung cancer cells. (a and b) Pearson correlation analysis was utilized to assess the expression correlation of miR-214-3p with circCPA4 and TGIF2 in non-small cell lung cancer tissues. (c) The expression association between circCPA4 and TGIF2 was analyzed by Pearson's correlation analysis. (d–f) TGIF2 protein level was determined in A549 and NCI-H1299 cells transfected with si-NC, si-circCPA4#2, si-circCPA4#2 + miR-NC, and si-circCPA4#2 + miR-214-3p. (g) RT-qPCR analysis of circCPA4 expression in circCPA4 or vector-transfected A549 and NCI-H1299 cells. (h) Western blot analysis of TGIF2 protein level in A549 and NCI-H1299 cells transfected miR-NC, miR-214-3p, miR-214-3p + vector, and miR-214-3p + circCPA4. Data are presented as mean  $\pm$  SD,  $n = 3$ . \*\*\* $p < 0.001$

**FIGURE 5** Overexpression of TGIF2 abolished the effects of circCPA4 knockdown on colony formation, migration, invasion, cell cycle progression, apoptosis, and autophagy in lung cancer cells. (a and b) Both mRNA level and protein level of TGIF2 were measured in TGIF2 or pcDNA-transfected A549 and NCI-H1299 cells. (c–m) A549 and NCI-H1299 cells were transfected with si-NC, si-circCPA4#2, si-circCPA4#2 + pcDNA, and si-circCPA4#2 + TGIF2. (c–e) Expression levels of TGIF2 were examined in transfected A549 and NCI-H1299 cells. (f) Number of colonies in transfected A549 and NCI-H1299 cells was determined. (g and h) Migration and invasion in transfected A549 and NCI-H1299 cells were assessed. (i) Apoptosis rate in transfected A549 and NCI-H1299 cells was examined. (j and k) Cell cycle distribution in transfected A549 and NCI-H1299 cells was measured. (l and m) Protein levels of Beclin1 and p62 in transfected A549 and NCI-H1299 cells were evaluated. Data are presented as mean  $\pm$  SD,  $n = 3$ . \*\* $p < 0.01$ , \*\*\* $p < 0.001$



**FIGURE 7** The effects of circCPA4 on tumor growth in lung cancer cells in vivo. (a and b) Tumor volume and tumor weight were examined in xenografts. (c) The RNA levels of circCPA4, miR-214-3p, and TGIF2 were detected in xenografted tumors by RT-qPCR assay. (d) TGIF2 protein level was measured in xenografted tumors by western blot assay. (e) The expression of ki-67 and TGIF2 was examined by using immunohistochemical staining of sections from the lung cancer xenograft model in nude mice. (f and g) Tumor volume and weight were determined in xenografts. (h and i) circCPA4, miR-214-3p, and TGIF2 expression were detected in xenografted tumors by RT-qPCR and western blot assay. (j) TGIF2 and ki-67 expression were examined using immunohistochemical staining of sections from the lung cancer xenograft model in nude mice. Data are presented as mean  $\pm$  SD. \* $p < 0.05$ , \*\* $p < 0.01$ , \*\*\* $p < 0.001$

NCI-H1299 cells. Additionally, the pcDNA-TGIF2 could attenuate si-circCPA4#2-triggered increase in Beclin1 protein level, and decrease in p62 protein level in A549 and NCI-H1299 cells (Figure 5l,m). Collectively, these results showed that circCPA4 could affect the progression of lung cancer partly through regulating TGIF2.

### CircCPA4 modulated TGIF2 expression through sponging miR-214-3p

In NSCLC tissues, we found that the expression level of miR-214-3p was negatively correlated with circCPA4 or TGIF2 (Figure 6a,b). Of interest, circCPA4 level was positively related to TGIF2 level in NSCLC cancer tissues (Figure 6c). After that, rescue assays showed that the down-regulation of miR-214-3p partially abolished the negative

effect of si-circCPA4#2 on TGIF2 protein level in A549 and NCI-H1299 cells (Figure 6d-f). In addition, the over-expression efficiency of circCPA4 was measured and exhibited in Figure 6g, and western blot assay suggested that the upregulation of circCPA4 could partly overturn the repression of miR-214-3p mimic on TGIF2 protein level in A549 and NCI-H1299 cells (Figure 6h). All in all, circCPA4 could act as a sponge of miR-214-3p to regulate TGIF2 expression.

### CircCPA4 silencing inhibited tumor growth in lung cancer cells in vivo

Finally, to prove the effect of circCPA4 deficiency on the tumorigenesis of lung cancer in vivo, a mouse xenograft model was established. As indicated in Figure 7a,b, the

depletion of circCPA4 could impede tumor growth, presenting as the decrease of tumor volume and tumor weight in circCPA4-knockdown mouse xenografts. RT-qPCR assays suggested that the levels of circCPA4 and TGIF2 were declined, and miR-214-3p was increased in tumor tissues from sh-circCPA4-transfected NCI-H1299 cell cells (Figure 7c). Apart from that, the TGIF2 protein level was also lower in the sh-circCPA4 group than the sh-NC group (Figure 7d). Besides, Immunohistochemical staining exhibited that the expression of TGIF2 and ki-67 (proliferation-related marker) was inhibited by circCPA4 down-regulation in this xenograft (Figure 7e). Additionally, our data also verified that the stable overexpression of circCPA4 could promote tumor growth in this xenograft model in nude mice (Figure 7f,g). Meanwhile, the significant upregulation of circCPA4 and TGIF2 was viewed in the sh-circCPA4 group, while miR-214-3p exhibited an opposite trend (Figure 7h,i). In addition, TGIF2 and ki-67 expression were increased in the circCPA4 overexpression group using Immunohistochemical staining assay (Figure 7j). These data disclosed that the knockdown of circCPA4 could retard tumor growth of lung cancer in vivo.

## DISCUSSION

To date, with the development of RNA sequencing technologies, an increasing number of circRNAs have been identified.<sup>28</sup> In recent years, circRNAs were considered as potential attractive biomarkers in human cancer due to the special structure and wide distribution.<sup>29,30</sup> In fact, previous studies revealed the regulatory roles of circRNAs in the development and progression of many tumors, including lung cancer.<sup>31–33</sup> Here, the high expression of circCPA4 was verified in lung cancer, in line with former studies.<sup>11</sup> Interestingly, this study verified circCPA4 might act as a promising biomarker in lung cancer on account of the stable loop structure. Functional analysis suggested that the knockdown of circCPA4 inhibited cell growth and metastasis of lung cancer cells. It has been acknowledged that the activation of apoptosis and autophagy could induce cell death, thereby suppressing the development of lung cancer.<sup>34,35</sup> In this study, our data showed the acceleration role of circCPA4 down-regulation on apoptosis and autophagy in lung cancer cells. Apart from that, the repression effect of circCPA4 deficiency on tumor growth was also validated in the mouse model. Thus, we considered that circCPA4 might exert a carcinogenic factor in lung cancer cells in vitro and in vivo.

Furthermore, it has previously been documented that TGIF2 plays a vital role in tumorigenesis by serving as an oncogene gene in lung adenocarcinoma, glioma, and osteosarcoma.<sup>36,37</sup> In this study, the TGIF2 level was increased in lung cancer. Further analysis verified the downregulation of TGIF2 blocked cell growth, metastasis, and facilitated autophagy of lung cancer cells, in agreement with the function of circCPA4 knockdown. Therefore, we then explored the relationship between circCPA4 and TGIF2 in lung cancer cells.

At present, the competing endogenous RNAs (ceRNAs) hypothesis proposes that circRNAs can isolate miRNAs which terminates the regulation of target mRNAs.<sup>38,39</sup> Hence, we further investigated whether the relationship between circCPA4 and TGIF2 was mediated by special miRNA. In this study, we predicted that there was an underlying binding between miR-214-3p and circCPA4 or TGIF2, and further verified their interaction in lung cancer cells. Moreover, miR-214-3p has been indicated as a tumor suppressor in lung cancer.<sup>19,40</sup> Low expression of miR-214-3p has been seen in NSCLC tissues and cells. As expected, miR-214-3p was inversely associated with circCPA4 or TGIF2 in NSCLC tissues. What is more, this study confirmed that the downregulation of miR-214-3p could reverse the inhibitory effect of circCPA4 knockdown on the expression level of TGIF2, further suggesting the circCPA4/miR-214-3p/TGIF2 axis in lung cancer. In addition, rescue assays manifested that the suppression impact of circCPA4 silencing on lung cancer progression was abolished by the upregulation of TGIF2, supporting the regulatory role of circCPA4 could be mediated by the miR-214-3p/TGIF2 axis in lung cancer progression.

Taken together, this study demonstrated that circCPA4 could act as a ceRNA of miR-214-3p to increase TGIF2 expression, thereby boosting the progression of lung cancer. Our findings provided an underlying circRNA-targeted therapy for lung cancer.

## ACKNOWLEDGMENTS

This study was supported by Key Research Projects of Natural Science in Colleges and Universities of Anhui Province (No. KJ2018A0858).

## CONFLICT OF INTEREST

The authors declare that they have no competing interest.

## ORCID

Wenhu Tao  <https://orcid.org/0000-0001-8204-2818>

## REFERENCES

1. Siegel RL, Miller KD. Cancer statistics, 2020. *CA Cancer J Clin*. 2020; 70:7–30.
2. O’Keeffe LM, Taylor G. Smoking as a risk factor for lung cancer in women and men: a systematic review and meta-analysis. *BMJ Open*. 2018;8:e021611.
3. Schuller HM. The impact of smoking and the influence of other factors on lung cancer. *Expert Rev Respir Med*. 2019;13:761–9.
4. Isaka M, Kojima H, Takahashi S, Omae K, Ohde Y. Risk factors for local recurrence after lobectomy and lymph node dissection in patients with non-small cell lung cancer: implications for adjuvant therapy. *Lung Cancer*. 2018;115:28–33.
5. Kristensen LS, Andersen MS, Stagsted LVW, Ebbesen KK, Hansen TB. The biogenesis, biology and characterization of circular RNAs. *Nat Rev Genet*. 2019;20:675–91.
6. Guo JU, Agarwal V, Guo H, Bartel DP. Expanded identification and characterization of mammalian circular RNAs. *Genome Biol*. 2014; 15:409.
7. Memczak S, Jens M, Elefsinioti A, Torti F, Krueger J, Rybak A, et al. Circular RNAs are a large class of animal RNAs with regulatory potency. *Nature*. 2013;495:333–8.

8. Liu W, Ma W, Yuan Y, Zhang Y, Sun S. Circular RNA hsa\_circRNA\_103809 promotes lung cancer progression via facilitating ZNF121-dependent MYC expression by sequestering miR-4302. *Biochem Biophys Res Commun.* 2018;500:846–51.
9. Gao S, Yu Y, Liu L, Meng J, Li G. Circular RNA hsa\_circ\_0007059 restrains proliferation and epithelial-mesenchymal transition in lung cancer cells via inhibiting microRNA-378. *Life Sci.* 2019;233:116692.
10. Peng H, Qin C. circCPA4 acts as a prognostic factor and regulates the proliferation and metastasis of glioma. *J Cell Mol Med.* 2019;23:6658–65.
11. Hong W, Xue M, Jiang J, Zhang Y, Gao X. Circular RNA circ-CPA4/let-7 miRNA/PD-L1 axis regulates cell growth, stemness, drug resistance and immune evasion in non-small cell lung cancer (NSCLC). *J Exp Clin Cancer Res.* 2020;39:149.
12. Zou J, Wu K, Lin C, Jie ZG. LINC00319 acts as a microRNA-335-5p sponge to accelerate tumor growth and metastasis in gastric cancer by upregulating ADCY3. *Am J Physiol Gastrointest Liver Physiol.* 2020;318:G10–22.
13. Ebrahimi SO, Reisi S. Downregulation of miR-4443 and miR-5195-3p in ovarian cancer tissue contributes to metastasis and tumorigenesis. *Arch Gynecol Obstet.* 2019;299:1453–8.
14. Saliminejad K, Khorram Khorshid HR, Soleymani Fard S, Ghaffari SH. An overview of microRNAs: biology, functions, therapeutics, and analysis methods. *J Cell Physiol.* 2019;234:5451–65.
15. Wang D, Gu J, Wang T, Ding Z. OncomiRDB: a database for the experimentally verified oncogenic and tumor-suppressive microRNAs. *Bioinformatics.* 2014;30:2237–8.
16. Han B, Ge Y, Cui J, Liu B. Down-regulation of lncRNA DNAJC3-AS1 inhibits colon cancer via regulating miR-214-3p/LIVIN axis. *Bioengineered.* 2020;11:524–35.
17. Yao X, Wu L, Gu Z, Li J. LINC01535 promotes the development of osteosarcoma through modulating miR-214-3p/KCNC4 Axis. *Cancer Manag Res.* 2020;12:5575–85.
18. Zou Y, Sun Z, Sun S. LncRNA HCG18 contributes to the progression of hepatocellular carcinoma via miR-214-3p/CENPM axis. *J Biochem.* 2020;168:535–46.
19. Yang Y, Li Z, Yuan H, Ji W, Wang K, Lu T, et al. Reciprocal regulatory mechanism between miR-214-3p and FGFR1 in FGFR1-amplified lung cancer. *Oncogenesis.* 2019;8:50.
20. Tang Q, Zheng F, Liu Z, Wu JJ, Chai XS, He CX, et al. Novel reciprocal interaction of lncRNA HOTAIR and miR-214-3p contribute to the solamargine-inhibited PDPK1 gene expression in human lung cancer. *J Cell Mol Med.* 2019;23:7749–61.
21. Liu C, Yi X. miR-541 serves as a prognostic biomarker of osteosarcoma and its regulatory effect on tumor cell proliferation, migration and invasion by targeting TGIF2. *Diagn Pathol.* 2020;15:96.
22. Jiang J, Wu RH, Zhou HL, Li ZM, Kou D, Deng Z, et al. TGIF2 promotes cervical cancer metastasis by negatively regulating FCMR. *Eur Rev Med Pharmacol Sci.* 2020;24:5953–62.
23. Du R, Shen W. TGIF2 promotes the progression of lung adenocarcinoma by bridging EGFR/RAS/ERK signaling to cancer cell stemness. *Signal Transduct Target Ther.* 2019;4:60.
24. Lu YJ, Liu RY, Hu K, Wang Y. MiR-541-3p reverses cancer progression by directly targeting TGIF2 in non-small cell lung cancer. *Tumour Biol.* 2016;37:12685–95.
25. Pang L, Cheng Y, Zou S, Song J. Long noncoding RNA SNHG7 contributes to cell proliferation, migration, invasion and epithelial to mesenchymal transition in non-small cell lung cancer by regulating miR-449a/TGIF2 axis. *Thorac Cancer.* 2020;11:264–76.
26. Jiang G, Wu AD, Huang C, Gu J, Zhang L, Huang H, et al. Isorhapontigenin (ISO) inhibits invasive bladder cancer formation in vivo and human bladder cancer invasion in vitro by targeting STAT1/FOXO1 Axis. *Cancer Prev Res (Phila).* 2016;9:567–80.
27. Ryter SW, Choi AM. Autophagy in lung disease pathogenesis and therapeutics. *Redox Biol.* 2015;4:215–25.
28. López-Jiménez E, Rojas AM, Andrés-León E. RNA sequencing and prediction tools for circular RNAs analysis. *Adv Exp Med Biol.* 2018;1087:17–33.
29. Chen B, Huang S. Circular RNA: an emerging non-coding RNA as a regulator and biomarker in cancer. *Cancer Lett.* 2018;418:41–50.
30. Huang X, Zhang W. Prognostic and diagnostic significance of circRNAs expression in lung cancer. *Adv Exp Med Biol.* 2019;234:18459–65.
31. Yu H, Chen Y, Jiang P. Circular RNA HIPK3 exerts oncogenic properties through suppression of miR-124 in lung cancer. *Biochem Biophys Res Commun.* 2018;506:455–62.
32. Ma X, Yang X, Bao W, Li S, Liang S, Sun Y, et al. Circular RNA circMAN2B2 facilitates lung cancer cell proliferation and invasion via miR-1275/FOXK1 axis. *Biochem Biophys Res Commun.* 2018;498:1009–15.
33. Han W, Wang L, Zhang L, Wang Y, Li Y. Circular RNA circ-RAD23B promotes cell growth and invasion by miR-593-3p/CCND2 and miR-653-5p/TIAM1 pathways in non-small cell lung cancer. *Biochem Biophys Res Commun.* 2019;510:462–6.
34. Liu H, Wei S, Zhang L, Yuan C, Duan Y, Wang Q. Secreted Phosphoprotein 1 promotes the development of small cell lung cancer cells by inhibiting autophagy and apoptosis. *Pathol Oncol Res.* 2019;25:1487–95.
35. Maheswari U, Ghosh K, Sadras SR. Licarin a induces cell death by activation of autophagy and apoptosis in non-small cell lung cancer cells. *Apoptosis.* 2018;23:210–25.
36. Xi L, Zhang Y, Kong S, Liang W. miR-34 inhibits growth and promotes apoptosis of osteosarcoma in nude mice through targetly regulating TGIF2 expression. *Biosci Rep.* 2018;38:BSR20180078.
37. Diao Y, Jin B, Huang L, Zhou W. MiR-129-5p inhibits glioma cell progression in vitro and in vivo by targeting TGIF2. *J Cell Mol Med.* 2018;22:2357–67.
38. Zhong Y, Du Y, Yang X, Mo Y, Fan C, Xiong F, et al. Circular RNAs function as ceRNAs to regulate and control human cancer progression. *Mol Cancer.* 2018;17:79.
39. Meng X, Li X, Zhang P, Wang J, Zhou Y, Chen M. Circular RNA: an emerging key player in RNA world. *Brief Bioinform.* 2017;18:547–57.
40. Lu T, Yang Y, Li Z, Lu S. MicroRNA-214-3p inhibits the stem-like properties of lung squamous cell cancer by targeting YAPI. *Cancer Cell Int.* 2020;20:413.

**How to cite this article:** Tao W, Cao C, Ren G, Zhou D. Circular RNA circCPA4 promotes tumorigenesis by regulating miR-214-3p/TGIF2 in lung cancer. *Thorac Cancer.* 2021;12:3356–69. <https://doi.org/10.1111/1759-7714.14210>